Journal of Applied Polymer Science

Effect of Polymer Structure on the Morphologies and Dielectric Properties of Nanoporous Polyimide Films

Fengzhu Lv, Leipeng Liu, Yihe Zhang, Penggang Li
National Laboratory of Mineral Materials, School of Materials Science and Technology,
China University of Geosciences (Beijing), Beijing 100083, China
Correspondence to: F. Z. Lv (E-mail: lfz619@cugb.edu.cn) and Y. H. Zhang (E-mail: zyh@cugb.edu.cn)

ABSTRACT: Low dielectric constant polyimide (PI) films have potential applications in integrated circuit. In this study, poly(methyl methacrylate), poly(ethylene oxide), and polystyrene as thermally labile materials were used as templates to generate PI films with nanopores by first mixing the polymer templates with the precursor of PI, poly(amic acid), followed by imidization of poly(amic acid) together with degradation of the polymer templates. The sizes of the formed pores, the thermal and dielectric constant of the nanofoamed PI films were studied and compared in detail. It is concluded that the dielectric constant of PI films using poly(ethylene oxide) as pore template is more stable because of the formation of uniform pores which is from the great accordance of imidization temperature of poly(amic acid) with the degradation temperature of poly(ethylene oxide). But that using poly(methyl methacrylate) as pore template is frequency dependent as the influence of inhomogeneous pores and PMMA residue from incompletely degradation of poly(methyl methacrylate). © 2014 Wiley Periodicals, Inc. J. Appl. Polym. Sci. **2015**, *132*, 41480.

KEYWORDS: dielectric properties; polyimides; porous materials

Received 4 May 2014; accepted 2 September 2014
DOI: 10.1002/app.41480

INTRODUCTION

As integrated circuit (IC) dimensions continue to decrease, device performances do not necessarily decrease accordingly because of the substantial increases in interconnect delays, cross-talk noise, and power dissipation.[1–3] Materials that possess low dielectric (low-k) constant are being developed to replace the general dielectric material, silicon dioxide (dielectric constant = 3.5), as the interlevel dielectric. The specifications for insulating films of the next generation of IC are that their dielectric constant should approach or below 2.0.[4,5] Because most solid materials have relatively high dielectric constant, one way of preparing low-k materials is introduction voids into the solid materials to take advantage of the lowest dielectric constant of air (dielectric constant =1). Such nanoporous and mesoporous materials have attracted tremendous amount of interests for application in IC devices for microelectronics technologies. [6–10]

Polyimide (PI) derived from pyromellitic dianhydride (PMDA) and oxydianiline (ODA) has been proved to be the most suitable high performance polymer for microelectronic applications because of its process ability in the poly(amic acid) (PAA) precursor form and excellent properties after thermal curing because of the semi-rigid aromatic structure.[11] Therefore, considerable attentions have been focused on the preparation of low-dielectric porous PI films with pore size ranging from angstroms to micrometers.

Methods for preparation of porous PIs include high temperature processing, nonsolvent induced phase separation,[12] vapor induced phase separation,[13–15] sacrifice template, embedding porous filler, such as porous additive carbon,[16] polysilsesquioxane and its derivatives, among which sacrifice template is the widely used method. The templates generally used are SiO_2 and thermal labile polymers.[17–20] Polymers containing poly(methyl methacrylate) (PMMA),[21] polystyrene (PS),[22] poly(ethylene oxide) (PEO),[23,24] poly(ε-caprolactone) (PCL)[25]are used as templates of pores to form porous PI materials by simple blending, or grafting, or linking with the precursor of PI, poly(PAA, to produce phase separation in solution, followed by thermal imidization of PAA and removal of the templates. Although sacrifice template has been successfully used to prepare porous PI films at the nanometer to micrometer length scale, the structure contribution of the degradation part to the pores and the dielectric properties of PI films have not been clarified.

In this study, to avoid the complex synthesis of block copolymers, thermal labile homopolymers of PEO, PMMA, and PS with almost the same molecular weight were used as templates of pores to prepare nanoporous PI films to study the contribution of different structure to the pore size, thermal stability, and

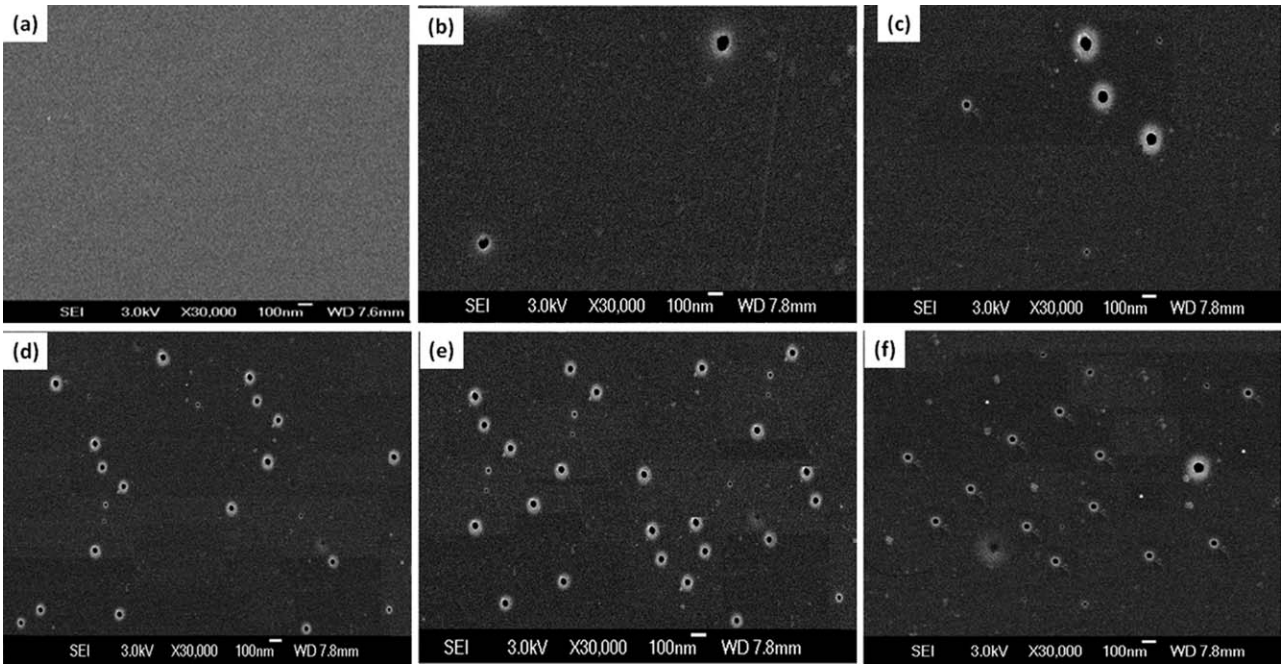

Figure 1. Cross-sectional SEM images of (a) PI and nanofoamed PI films from PAA-PEO with (b) 1, (c) 3, (d) 5, (e) 7, and (f) 10 wt % of PEO.

dielectric properties of PIs. The sizes of the formed pores, the thermal and dielectric constant of the nanoporous PI films were studied and compared in detail. Although PMMA (with carboxyl group) and PS (with benzyl group) were more structural similar to PAA, but PEO was more suitable as template for producing uniform pores to lower the dielectric constant of PI films.

EXPERIMENTAL

Materials

PMDA and ODA from Hangzhou Taida and Beijing Chemical Reagen,China, respectively, were dehydrated prior to use. *N,N*-Dimethylacetamide (DMAc, analytical grade) from Beijing Yili Chemicals Reagen was dried over molecular sieves before use. PEO was purchased from Beijing Guoren Yikang, Beijing, China, and dried prior to use. PMMA and PS were from Beijing haier ke hua and dried prior to use.

Preparation of PI Films

PAA precursor for PI films was prepared by polymerizing of PMDA and ODA in DMAc. The procedure was performed by initially adding desired amount of PMDA to DMAc to ensure complete dissolution and then adding 1.01 equivalent molar amount of ODA. The solution was then stirred at 0°C for 8 h to give a viscous solution. Then PEO (or PMMA, or PS) was dissolved in little DMAc, respectively, and then slowly added to the above viscous system. The mixture was then stirred continuously for 6 h at room temperature. Then the PAA-PEO (or PAA-PMMA, or PAA-PS) films were prepared by casting the viscous liquid onto a glass plate and then dried at room temperature for 1 h. For further drying, the films were heated at 80°C, 120°C, and 150°C for 1 h, respectively, then thermal imidized at 250°C and 300 °C for 0.5 h, respectively, to obtain light yellow transparent films.[26] The final PI films from PAA-PEO, PAA-PMMA, and PAA-PS were assigned as PI-PEO, PI-PMMA, and PI-PS, respectively.

Characterization

The cross-sectional images of the PI nanoporous films were taken by field emission SEM (JEOL JSM-6335F) operating at 15 kV. The thermal stability of the PI nanoporous films was studied by TGA (HCT-2, Beijing, China) in a nitrogen atmosphere at a heating rate of 10°C/min. The dielectric constant was measured using a frequency-response dielectric analyzer (Novocontrol Alpha-analyzer) at different temperatures in a frequency range of 1 Hz−10 MHz. All the dielectric measurements were conducted under a nitrogen flow (20 mL/min) and the sample thicknesses were between 30 to 40 μm. Dynamic mechanical analysis measurements were performed using a DMS6100 in the tension mode over a temperature range from 25°C to 400°C. Data acquisition and analysis of the storage modulus (E') and loss tangent (tan θ) were recorded automatically by the system. The heating rate and frequency were fixed at 10°C/min and 1 Hz, respectively.

RESULTS AND DISCUSSION

Morphology of Nanoporous PI-PEO, PI-PMMA, and PI-PS Films

Figures 1 show the cross-sectional SEM images of pure PI, PI-PEO (Figure 1), PI-PMMA (Figure 2), and PI-PS (Figure 3) films with different content of PEO, PMMA, and PS, respectively. The white areas in the SEM images are closed voids from the degraded PEO, PMMA, and PS phase. The porous structure of the nanoporous films can be clearly observed as compared to pure PI film [Figure 1(a)]. The observed closed voids are in a size range of 40–200 nm, with a very smaller part of

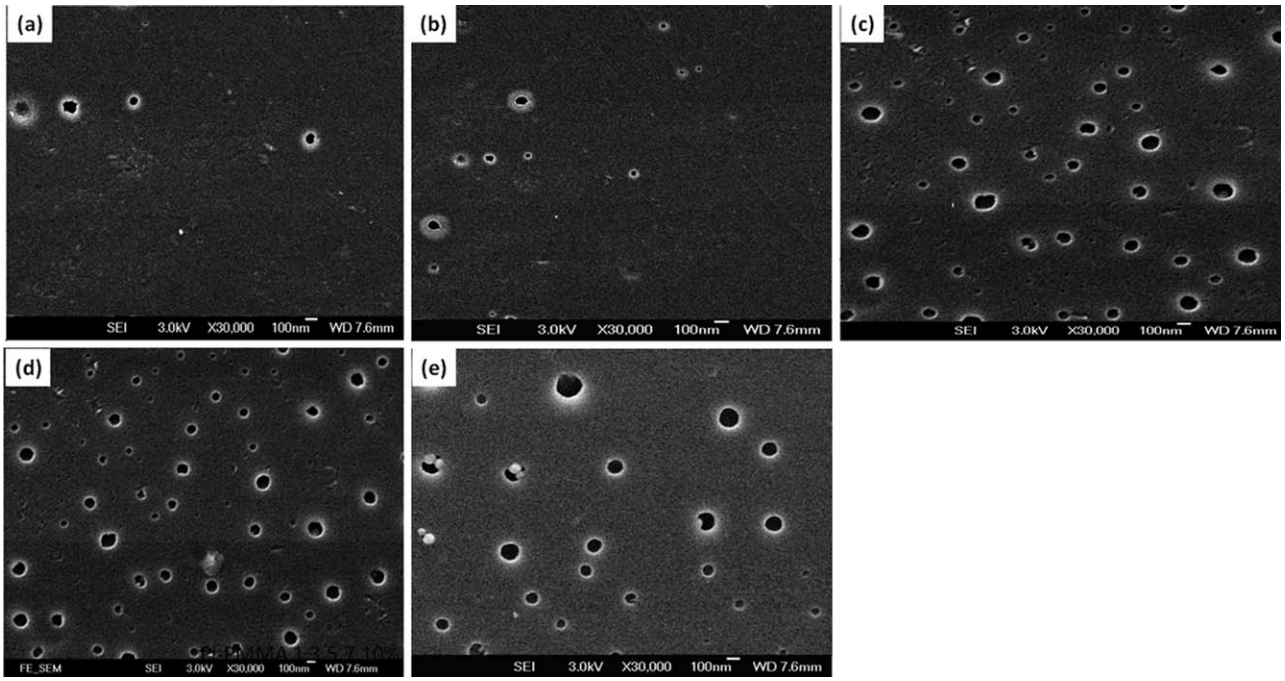

Figure 2. Cross-sectional SEM images of nanofoamed PI films from PAA-PMMA with (a) 1, (b) 3, (c) 5, (d) 7, and (e) 10 wt % of PMMA.

interconnected ones. In all of the three kinds of nanoporous PI films, especially in nanoporous PI-PMMA and PI-PS films, nonspherical voids are observed. The deviation of the voids away from the expected spherical morphology is because of the stress and high pressure as smaller molecules from the thermal decomposition of PEO, PMMA, and PS escaping from the PI matrix during the imidization process. Also when small molecules escape from the films, interconnected channels are left. Comparison the SEM photographs of the three kinds of nanoporous films, it is clear that under the same content of polymer templates in PAA, the formed nanoporous films of PI-PMMA (Figure 2) contain the highest pore size variation, while the pore size of PI-PEO (Figure 1) almost does not change. The pore size variation of PI-PS is in the middle of the three kinds (Figure 3). So the pores of the nanoporous PI-PEO is more uniform than PI-PMMA and PI-PS under the same content of

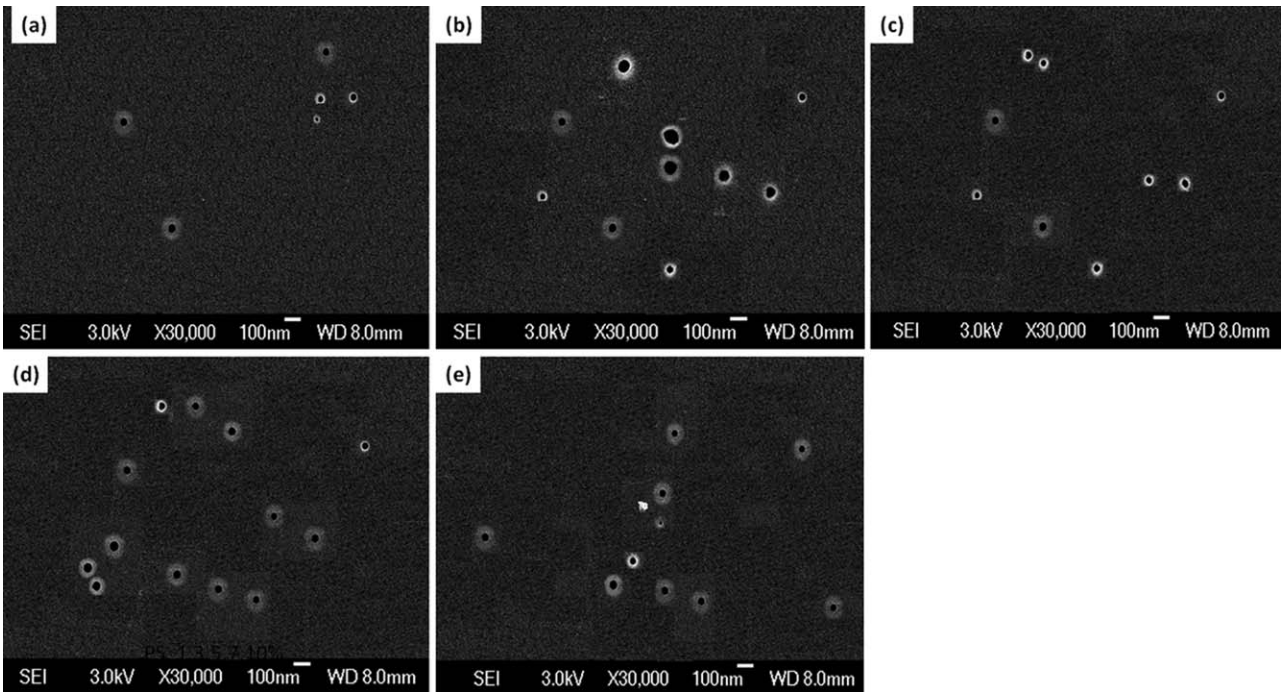

Figure 3. Cross-sectional SEM images of nanofoamed PI films from PAA-PS with (a) 1, (b) 3, (c) 5, (d) 7, and (e) 10 wt % of PS.

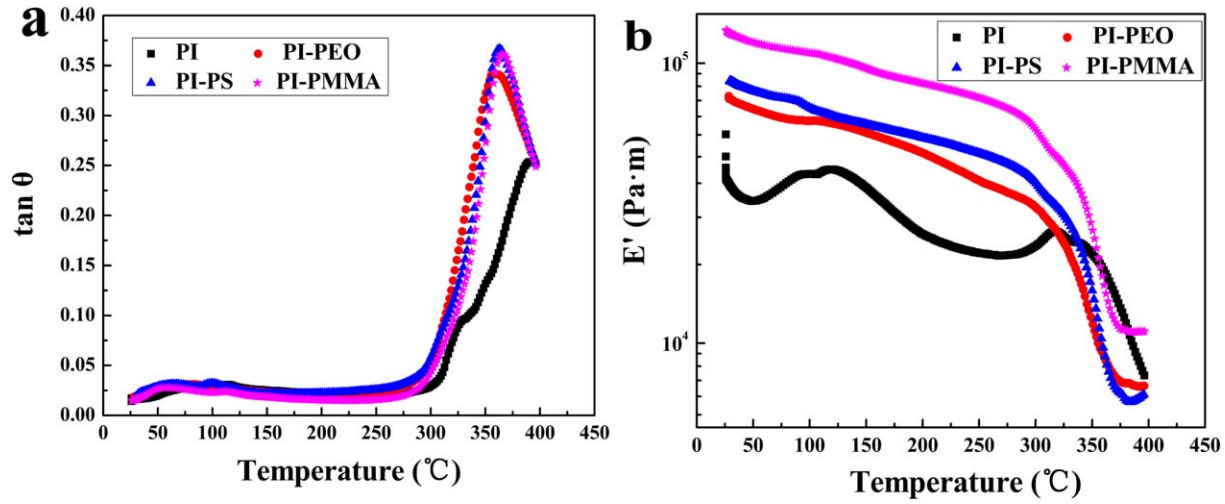

Figure 4. (a) Mechanical loss factors and (b) storage modulus of the pure PI and nanofoamed PI as a function of temperature. [Color figure can be viewed in the online issue, which is available at wileyonlinelibrary.com.]

voids. The degradation of PEO, PS, and PMMA in air are in the range of 200–400°C (uniformly decompose),[23] 307–380°C (mainly 362°C),[27] and 242–392°C.[28] The thermal imidization of PAA is at 250°C and 300°C for 0.5 h. So the first stage imidization temperature of PAA (250°C for 0.5 h) is higher than the beginning degradation temperature of PEO, while almost equal to the beginning degradation temperature of PMMA. But the beginning degradation temperature of PS is even slightly higher than the final imidization temperature (300°C for 0.5 h). It can be inferred that at the beginning of imidization, PEO and PMMA begin to degrade. But at this temperature only part of PAA are imidized and the viscosity of the system is low, so the smaller molecules from PEO and PMMA degradation can easily escape from the system and can only slightly reinforce the shape change of the pores. But the degradation range of PEO and PMMA is broad which means at the first imidization stage only part of PEO and PMMA are degraded. At higher imidization temperature (stage 2), the release of small molecules from PMMA in the same time is more than that of PEO, since its degradation temperature is narrow. So the stress and pressure in PI-PMMA is larger than that in PI-PEO and irregular pores can be easily formed. The porous structure of the target PI films is based on the decomposition of the thermally labile material (PMMA, PS, PEO) phase. In order to prevent the collapse of the porous structure it is essential that the thermally decomposition temperature of the labile material is below the *Tg* of the PI matrix. It can be seen from Figure 4(a) that the *Tg* of pure PI film is 391°C, that is higher than the porous PI which is ~360°C. But these *Tg* are all higher than the decomposition temperature of PMMA, PS, and PEO. The degradation of PS is in the second imidization stage and lower than the *Tg* of PI. So the viscosity of the system that PS degradation may be large. The small molecules from PS degradation are difficult to escape from the film. Irregular viods are easy to be formed. Although PMMA (carboxyl group) and PS (benzyl group) are more compatible with PAA than PEO because of the structure and group similarity of the two polymers with PAA, but PEO was more suitable as template to produce uniform pores because of the suitable degradation temperature.

According to the above analysis, it is preferred that PEO and PMMA may be completely degraded in the imidization process. While PS residue is left in the film. In order to confirm this inference the thermal stability of the films are studied.

Dynamical Mechanical Properties of PI-PEO, PI-PMMA, and PI-PS Nanoporous Films

The storage modulus and tan θ as a function of temperature are shown in Figure 4. The storage modulus of the pristine PI decreased with increasing temperature at lower temperature and increase near *Tg*. When the temperature is higher than the *Tg*, the polymeric matrix begins to transit from glassy to elastic state, and the storage modulus falls rapidly.[29] the storage modulus of nanoporous PIs are all higher than pristine PI because of the contribution of pores[30] which can limit the diffusion of forces. But the storage modulus of nanoporous PIs decrease almost linearly with temperature which is because of the callapes of pores. This phenomenon still indicates that the pores in the PI films are not uniform but polydisperse.

Thermal Stability of PI-PEO, PI-PMMA, and PI-PS Nanoporous Films

The TGA curves of dense PI film, PI-PMMA, PI-PS, and PI-PEO nanoporous films formed with 5 wt % polymer templates are shown in Figure 5. One obvious weight loss in the curve of PI-PMMA at 390–420°C is observed which may be the degradation of PMMA residue. The 5 wt % weight loss, which is always considered as the beginning decomposition temperature of polymers, of PI and PI-PEO, PI-PS, and PI-PMMA nanoporous films are 541.8°C, 528.0°C, 504.7°C, and 414.0°C. It can be seen that the thermal decomposition temperature of nanoporous PI films decreases with the formation of void by PEO, PMMA, and PS. The thermal stability of PI films decreases in the order of PI-PEO, PI-PS, and PI-PMMA. While the temperature for the rapid decomposition of the PI film framework is in

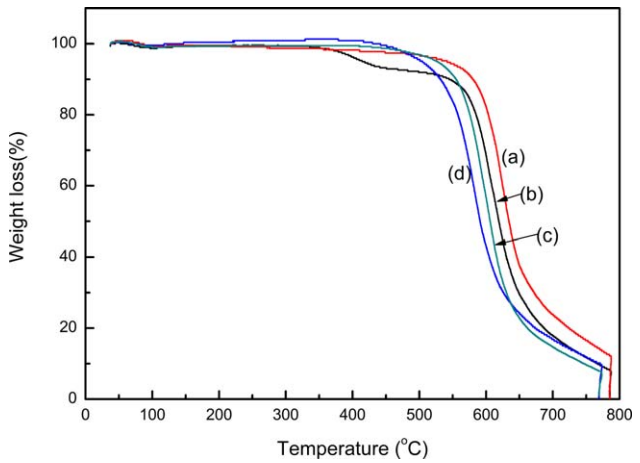

Figure 5. TGA curves of (a) dense PI film and (b) PI-PMMA, (c) PI-PS, and (d) PI-PEO nanofoamed films formed from precursors with 5 wt % polymer templates. [Color figure can be viewed in the online issue, which is available at wileyonlinelibrary.com.]

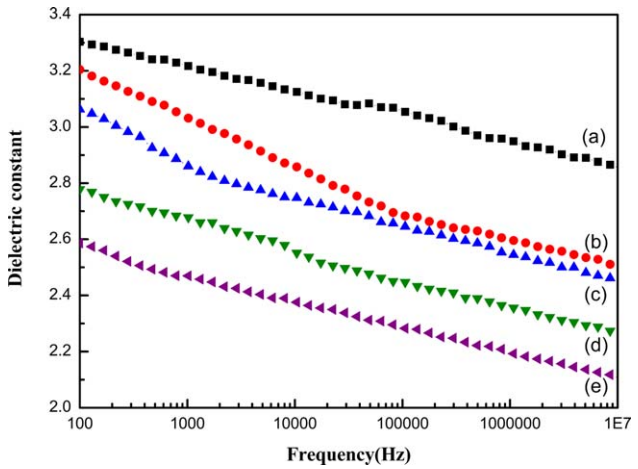

Figure 7. Dielectric constant of PI nanofoamed films as a function of frequency from precursors with (a) 1, (b) 3, (c) 5, (d) 7, and (e) 10 wt % of PS. [Color figure can be viewed in the online issue, which is available at wileyonlinelibrary.com.]

the order of PI> PMMA> PS>PEO. The order change confirms polymer residues exist in the films.

The TGA measurement indicates that in the imidization temperature PEO and PS degraded almost completely, but PMMA could only partly degraded. There are PMMA residues in the films.

Dielectric Properties of Nanoporous PI-PEO, PI-PMMA, and PI-PS

Figures 6–8 show the frequency dependence of the dielectric constant of the PI nanoporous films from precursors with various contents of PEO, PMMA, and PS. All the porous PI films exhibit lower dielectric constant compared to that of the pure PI film [Figure 6(a)], which is 3.3 at 100 Hz, because of the contribution of pores which increase the free volume of the films. The dielectric constant of all the films decreases with the increase of the template content since the free volume of the films is further increased because of more pores formed in the films.[31] Meanwhile the dielectric constant decrease with increasing frequency for all the samples. Maxwell–Wagner type polarization is known to be active at lower frequency that explains why a decrease of the dielectric constant is observed when the measurement frequency is increased.[32] That is, the polarity of the polar unit in PI film cannot follow the frequency change.[33] The dielectric constant decreases with increasing frequency for all the samples is in accord with the result of porous PI silica composite.[34]

At 100 Hz the dielectric constant of PI-PEO, PI-PS, and PS-PMMA from 5 wt % polymer templates are 2.74, 3.06, and 3.16. At 1×10^5 Hz the dielectric constant of the samples are 2.47, 2.65, and 2.75 accordingly. That is at lower frequency, the dielectric constant of PI-PEO is lower than that of PI-PS, and

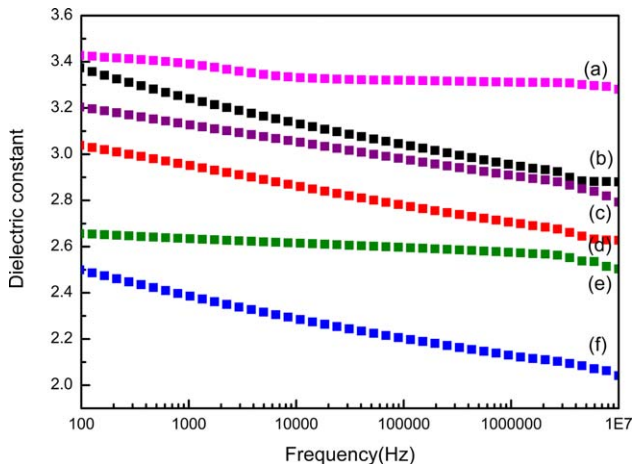

Figure 6. Dielectric constant of PI nanofoamed films as a function of frequency from the precursors with (a) 0, (b) 1, (c) 3, (d) 5, (e) 7, and (f) 10 wt % of PEO. [Color figure can be viewed in the online issue, which is available at wileyonlinelibrary.com.]

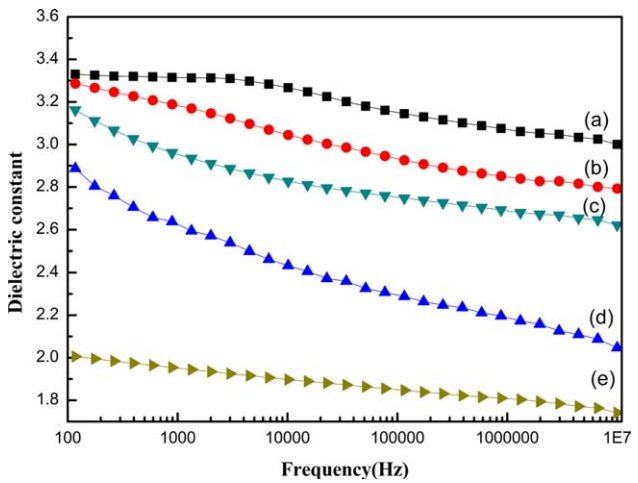

Figure 8. Dielectric constant of PI nanofoamed films as a function of frequency from precursors with (a) 1, (b) 3, (c) 5, (d) 7, and (e) 10 wt % of PMMA. [Color figure can be viewed in the online issue, which is available at wileyonlinelibrary.com.]

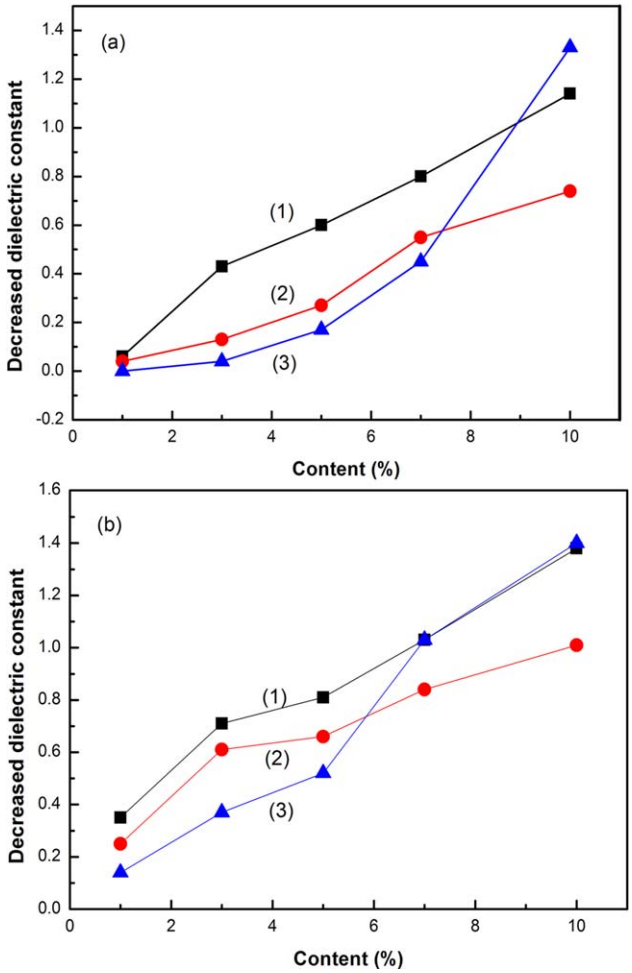

Figure 9. Decreased values of the dielectric constant of PI films at (a) 100 Hz and (b) 100,000 Hz using 5 wt % of (1) PEO, (2) PS, and (3) PMMA as porous templates. [Color figure can be viewed in the online issue, which is available at wileyonlinelibrary.com.]

then PS-PMMA. The decreased dielectric constant with content of polymer templates at 100 Hz and 1×10^5 Hz are summarized in Figure 9. It is clearly that no matter at 100 or 1×10^5 Hz, at low polymer template contents the decreased value of dielectric constant of the PI films increase in the order of PI-PMMA, PI-PS, and PI-PEO, while as the content of polymer template content increase to 10 wt %, the decreased dielectric constant value of PI-PMMA increase to the largest. This phenomenon indicates PI-PMMA is more frequency dependent. It is reported the dielectric constant of PMMA is lower than that of PS and PI.[33] So the great decreased values of PI-PMMA at 1×10^5 Hz are because of the irregular pores and the existence of PMMA residue. Therefore, the dielectric constant of PI films formed by using PEO as pore template is more stable.

CONCLUSIONS

In summary, nanoporous PI films are prepared by mixing PEO, PS, and PMMA with PAA from PMDA and ODA, respectively, and then imidization of PAA together with the degradation of the polymer templates. The formed pore sizes range in tens to hundreds of nanometers. The dielectric constant of the porous films decreases greatly with the introduction of pores. The thermal and dielectric constant of nanoporous PI films using PEO, PS, and PMMA as pore templates are compared in detail. The dielectric constant and thermal stability of PI-PEO is more stable while PI-PMMA is frequency dependent.

ACKNOWLEDGMENTS

The work was jointly supported by the Fundamental Research Funds for the Central Universities (2-9-2013-49) and the Project of Chinese Geological Survey (1212011120309).

REFERENCES

1. Chapelon, L. L.; Petitprez, E.; Brun, P.; Farcy, A.; Torres, J. *Microelectron. Eng.* **2007**, *84*, 2624.
2. Yu, M. B.; Ning, J.; Balakumar, S.; Bliznetsov, V. N.; Lo, G. Q.; Balasubramanian, N.; Kwong, D. L. *Thin Solid Films* **2006**, *504*, 257.
3. Chang, T. S.; Chang, T. C.; Liu, P. T.; Chiang, C. Y.; Chen, S. C.; Yeh, F. S. *Thin Solid Films.* **2006**, *515*, 1117.
4. Srikanth, N.; Tiong, L. C.; Vath, C. *J. Microelectron. Eng.* **2008**, *85*, 440.
5. Lee, K. H.; Lee, K.; Suk, M.; Choi, J. M.; Im, S.; Jang, S.; Kim, E. *Org. Electron.* **2009**, *10*, 194.
6. Chapelon, L. L.; Chaabouni, H.; Imbert, G.; Brun, P.; Mellier, M.; Hamioud, K.; Farcy, A.; Torres, J. *Microelectron. Eng.* **2008**, *85*, 2098.
7. Carter, K. R.; DiPietro, R. A.; Sanchez, M. I.; Swanson, S. A. *Chem. Mater.* **2001**, *13*, 213.
8. Mikoshiba, S.; Hayase, S. *J. Mater. Chem.* **1999**, *9*, 591.
9. Zhao, X. Y.; Liu, H. *J. Polym. Int.* **2010**, *59*, 597.
10. Krause, B.; Koops, G. H.; van der Vegt, N. F. A. *Adv. Mater.* **2002**, *14*, 1041.
11. Liaw, D. J.; Wang, K. L.; Huang, Y. C. *Prog. Polym. Sci.* **2012**, *37*, 907.
12. Pan, L. Y.; Zhan, M. S.; Wang, K. *Polym. Eng. Sci.* **2010**, *50*, 1261.
13. Takeichi, T.; Yamazaki, Y.; Ito, A.; Zuo, M. *J. Photopolym. Sci. Technol.* **1999**, *12*, 203.
14. Takeichi, T.; Yamazaki, Y. *J. Photopolym. Sci. Technol.* **2000**, *13*, 333.
15. Nguyen, T; Wang, X. *J. Power Sources* **2010**, *195*, 1024.
16. Im, J. S.; Bae, T. S.; Lee, S. K. *Mater. Res. Bull.* **2010**, *45*, 1641.
17. Jiang, L.; Liu, J.; Wu, D. *Thin Solid Films* **2006**, *510*, 241.
18. Zhang, Y.; Yu, L.; Su, Q. *J. Mater. Sci.* **2012**, *47*, 1958.
19. Wang, Q.; Wang, C.; Wang, T. *J. Colloid. Interf. Sci.* **2013**, *389*, 99.
20. Kim, W.; Lee, M. K. *Mater. Lett.* **2009**, *63*, 933.
21. Fu, G. D.; Zong, B. Y.; Kang, E. T. *Ind. Eng. Chem. Res.* **2004**, *43*, 6723.
22. Wang, T. M.; Wang, Q. H. *Express. Polym. Lett.* **2013**, *7*, 667.
23. Lee, Y. J.; Huang, J. M.; Kuo, S. W.; Chang, F. C. *Polymer* **2005**, *46*, 10056.

24. Zhang, Y. H.; Yu, L.; Zhao, L. H.; Tong, W. S.; Huang, H. T.; Ke, S. M. *J. Electron. Mater.* **2012**, *41*, 2281.

25. Ju, J. P.; Wang, Q. H.; Wang, T. M.; Wang, C. *J. Colloid Interface Sci.* **2013**, *404*, 36.

26. Zhang, Y.; Li, Y.; Li, G.; Huang, H.; Chan, H. L. W.; Daoud, W. A.; Li, L. *Chem. Mater.* **2007**, *19*, 1939.

27. Mosallamy, E.; El-Said, H. *J. Therm. Anal. Calorim.* **2014**, *115*, 707.

28. Fu, G. D; Wang, W. C.; Li, S.; Kang, E. T.; Neoh, K. G.; Liaw, D. J. *J. Mater. Chem.* **2003**, *13*, 2150.

29. Lin, J. J.; Wang, X. D. *Polymer* **2007**, *48*, 318.

30. Chang, C. J.; Tsai, M. H.; Chen, G. S.; Wu, M. S.; Hung, T. W. *Thin Solid Films* **2009**, *517*, 4966.

31. Kivilcim, N.; Seckin, T.; Koytepe, S. *J. Porous Mater.* **2013**, *20*, 709.

32. Li, Y.; Lu, X.; Liu, X. *Appl. Phys. A* **2010**, *100*, 207.

33. Shang, J. W.; Zhang, Y. H.; Yu, L.; Luan, X. L.; Shen, B.; Zhang, Z. L.; Lv, F. Z.; Chu, P. K. *J. Mater. Chem. A* **2013**, *1*, 884.

34. Wang, Q.; Wang, C.; Wang, T. *J. Colloid Interface Sci.* **2013**, *389*, 99.